Molecular Wires: Synthesis and Properties of the New Mixed-Valence Complex [Cp*(dppe)Fe−C≡C−X−C≡C−Fe(dppe)Cp*][PF_6] (X = 2,5 -C_4H_2S) and Comparison of Its Properties with Those of the Related All-Carbon-Bridged Complex (X = −C_4−)

Sylvie Le Stang, Frédéric Paul, and Claude Lapinte*

UMR CNRS 6509 Organométalliques et Catalyse, Université de Rennes I, Campus de Beaulieu, 35042 Rennes Cedex, France

Received October 18, 1999

The binuclear μ-bis(ethynyl)thiophene complex [Cp*(dppe)Fe−C≡C-2,5-C_4H_2S−C≡C−Fe-(dppe)Cp*] (**3**, Cp* = pentamethylcyclopentadienyl, dppe = 1,2-bis(diphenylphosphino)-ethane) was prepared in a three-step one-pot procedure from the 2,5-bis(trimethylsilylethynyl)-thiophene and the chloro organoiron complex Cp*(dppe)FeCl (**2**). Complex **3**, isolated as an orange thermally stable powder (72%), was characterized by ^{1}H, ^{13}C, and ^{31}P NMR, FTIR, UV−vis, and Mössbauer spectroscopies and elemental analysis. CV of **3** from −1.5 to 1.4 V vs SCE displayed two reversible one-electron waves with the (i_p^a/i_p^c) current ratio of unity. A third almost reversible process was observed at a more positive potential (i_p^a/i_p^c = 0.83, 0.100 V s^{-1} scan rate). The redox potentials E_0 are −0.39, −0.05, and 1.04 V vs SCE. The wave separation ($|\Delta E_0|$ = 0.34 V) between the two reversible oxidation processes leads to a big comproportionation constant ($K_c = 5.8 \times 10^5$), establishing the stability of the mixed-valence complex (MV). Addition of 0.95 equiv of [Cp_2Fe][PF_6] to a CH_2Cl_2 solution of **3** produces the MV Fe(II)−Fe(III) complex **4** (86%). Analytically pure samples in **4** were characterized by FTIR, Mössbauer, ESR, UV−vis, and NIR spectroscopies. It is established that the two metal sites in **4** are not equivalent on the very fast IR time scale (10^{-13} s). The Mössbauer spectrum of **4** shows the presence of a sharp unique doublet, indicating that the odd electron is delocalized on both metal centers on the Mössbauer time scale in the range $300 > T > 4$ K. In contrast, the Mössbauer spectrum of [Cp*(dppe)Fe−C≡C−C≡C−C≡C−C≡C−Fe(dppe)Cp*][PF_6] (**5**) displayed three doublets corresponding to Fe(II), Fe(III), and Fe(averaged), corresponding to the simultaneous presence of the trapped and detrapped valence in the same sample. The electronic coupling V_{ab} determined in CH_2Cl_2 is 2515 and 2520 cm^{-1} for the complexes **4** and **5**, respectively.

A molecular wire can be regarded as a one-dimensional molecule allowing through-bridge exchange of electrons (holes) between its remote terminal groups, themselves able to exchange electrons with the outside world.[1] This definition implies that the compounds must possess two redox active termini connected through a π-system allowing intramolecular electron transfer. It clearly appears from the literature reports that the properties of such compounds depend both on the redox termini and the spacer that connects them. Obviously, in this field, the challenge consists now not only in the synthesis of such extended one-dimensional molecules but also in the evaluation of their electron conduction capability. Indeed, despite the fact that a plethora of compounds with various redox termini and π-spacers have already been synthesized and presented as potential molecular wires, very few of these realizations were actually experimentally tested and evaluated for their electron conduction capability.[2−6]

The use of redox active organometallic building blocks assembled with all-carbon chains offers fascinating perspectives for the design and realization of such molecular wires. Several compounds with C_4 to C_{20} bridges were prepared and evaluated for their physical properties.[7−15] These compounds have shown a promizing potential for the development of new nanoscopic

* Corresponding author. E-mail: lapinte@univ-rennes1.fr.

(1) Lehn, J.-M. *Supramolecular Chemistry−Concepts and Perspectives*; VCH: Weinheim, 1995.
(2) Paul, F.; Lapinte, C. *Coord. Chem. Rev.* **1998**, *178−180*, 427.
(3) Lang, H. *Angew. Chem., Int. Ed. Engl.* **1994**, *33*, 547.
(4) Bunz, U. H. F. *Angew. Chem., Int. Ed. Engl.* **1996**, *35*, 969.
(5) Ward, M. D. *Chem. Ind.* **1997**, 640.
(6) Swager, T. M. *Acc. Chem. Res.* **1998**, *31*, 201.
(7) Le Narvor, N.; Lapinte, C. *J. Chem. Soc., Chem. Commun.* **1993**, 357.
(8) Le Narvor, N.; Toupet, L.; Lapinte, C. *J. Am. Chem. Soc.* **1995**, *117*, 7129.
(9) Guillemot, M.; Toupet, L.; Lapinte, C. *Organometallics* **1998**, *17*, 1928.
(10) Coat, F.; Guillevic, M.-A.; Toupet, L.; Paul, F.; Lapinte, C. *Organometallics* **1997**, *16*, 5988.
(11) Brady, M.; Weng, W.; Zhou, Y.; Seyler, J. W.; Amoroso, A. J.; Arif, A. M.; Böhme, M.; Frenking, G.; Gladysz, J. A. *J. Am. Chem. Soc.* **1997**, *119*, 775.
(12) Weng, W. Q.; Bartik, T.; Brady, M.; Bartik, B.; Ramsden, J. A.; Arif, A. M.; Gladysz, J. A. *J. Am. Chem. Soc.* **1995**, *117*, 11922.
(13) Falloon, S. B.; Szafert, S.; Arif, A. M.; Gladysz, J. A. *Chem. Eur. J.* **1998**, *4*, 1033.

10.1021/om9908231 CCC: $19.00
Publication on Web 02/16/2000

molecular devices. For instance, the [Cp*(dppe)Fe−C≡C−C≡C−C≡C−C≡C−Fe(dppe)Cp*][PF_6] displayed the strongest electronic coupling observed to date between two metal centers through nine bonds.[16] As the chain length increases, the synthesis becomes however more and more difficult and the stability of the compounds slowly decreases, especially with electron-rich termini. For this reason, we decided to synthesize new compounds incorporating cyclic groups chosen (i) to keep the rigid-rod geometry of the carbon chain, (ii) to facilitate the synthetic process, (iii) to increase the chemical stability of the compounds, and (iv) to maintain a high level of electronic coupling. Among the various π-conjugated systems developed during the past decade, thiophene and poly(thiophene) derivatives seem to present a blend of these properties.[17]

We now report the synthesis of the neutral binuclear complex Cp*(dppe)Fe−C≡C-2,5-C_4H_2S−C≡C−Fe(dppe)-Cp* (**3**) and the corresponding mixed-valence derivative [Cp*(dppe)Fe−C≡C-2,5-C_4H_2S−C≡C−Fe(dppe)Cp*][PF_6] (**4**). The thermodynamic stability (K_c), the rate of the intramolecular electron transfer, and the electronic coupling (V_{ab}) were also determined for **4**. The results are compared with those obtained for the known mixed-valence derivative [Cp*(dppe)Fe−C≡C−C≡C−C≡C−C≡C−Fe(dppe)Cp*][PF_6] (**5**),[16] for which the two iron centers are connected through a nine-bond bridge. For purpose of comparison, this study includes as well the Mössbauer spectroscopy and full UV−vis and NIR data for **5**, which were not previously reported.

Results and Discussion

Synthesis. The neutral binuclear μ-bis(ethynyl)-thiophene complex [Cp*(dppe)Fe−C≡C-2,5-C_4H_2S−C≡C−Fe(dppe)Cp*] (**3**) was obtained in a three-step one-pot procedure starting from the known bridging ligand 2,5-bis(trimethylsilylethynyl)thiophene (**1**)[18] and the chloro organoiron complex Cp*(dppe)FeCl (**2**,[19] Scheme 1). The reaction was carried out in methanol following a procedure previously described with specific modifications.[20] The first step consists of the cleavage of the trimethylsilyl groups by reacting **1** with 2 equiv of K_2CO_3. After 16 h of stirring, complex **2** is added together with $NaBPh_4$ (2.2 equiv) to facilitate the dissociation of the FeCl bond. In the last step the expected bis(vinylidene) derivative [Cp*(dppe)Fe=C=CH-2,5-C_4H_2S−HC=C=Fe(dppe)Cp*]2[BPh_4] was deprotonated, in situ, by KOBu^t (2 equiv). The complex **3** was then isolated in 89% yield as a pure orange powder. The presence of the triple bond was evidenced by the ^{13}C resonances of the quaternary carbon atoms at δ (C_6D_6) 139.2 ($^2J_{PC}$ = 40 Hz) and 112.9 and the characteristic IR frequencies (Table 1). The multiplicity of the triple-bond stretching mode is only observed in the solid state (Nujol). Note that for related iron alkynyl derivatives Cp*(dppe)Fe(C≡C−Ar), splittings had previously been attributed to Fermi coupling.[21−23] We do not believe that the splitting observed here has the same origin, since a single $\nu_{C\equiv C}$ vibration with a shoulder at 2032 cm^{-1} is present in the IR spectrum recorded in solution.[24]

Scheme 1

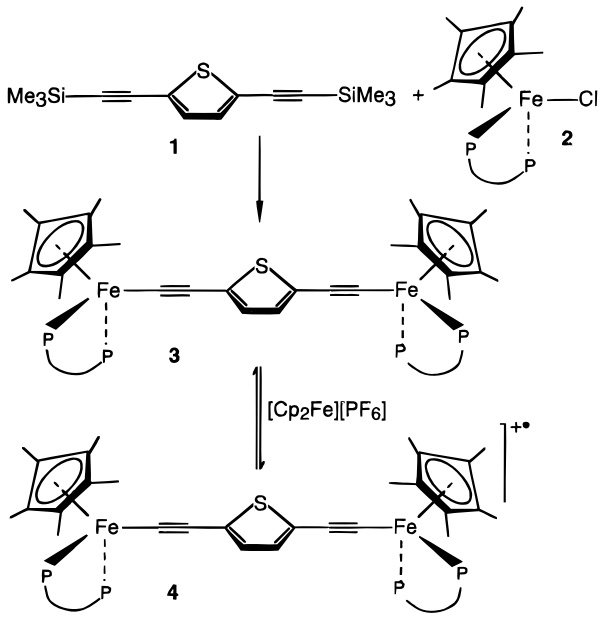

Table 1. IR $\nu_{C\equiv C}$ Bond Stretching[a] for the MV [Cp*(dppe)Fe−C≡C−X−C≡C−Fe(dppe)Cp*][PF_6]$_n$ (X = 2,5-C_4H_2S (4) and X = $-C_4-$ (5))[a] and the Related Neutral (n = 0) and Dicationic (n = 2) Derivatives

compd	n = 0	n = 1	n = 2
4	2054−2039 (2041)	1977 (1983) 1910 (1927)	1941 (1950)
5[b]	2109 (2092) 1949 (1934)	1879 (1881) 1784[c] (1808)[c]	2034−1884 1818

[a] Nujol (CH_2Cl_2), cm^{-1}. [b] From ref 16. [c] Very broad band.

Cyclic Voltammetry. The initial scan in the cyclic voltammogram of complex **3** from +1.4 to −1.5 V [vs standard calomel electrode (SCE)] is characterized by two reversible one-electron waves at E_0 = −0.39 and −0.05 V vs SCE (cf. ferrocene +0.460 V vs SCE)[25] in dichloromethane with an (i_p^a/i_p^c) current ratio of unity (Figure 1). These two waves correspond to the formation of [Cp*(dppe)Fe−C≡C-2,5-C_4H_2S−C≡C−Fe(dppe)Cp*]$^+$ and [Cp*(dppe)Fe−C≡C-2,5-C_4H_2S−C≡C−Fe(dppe)-Cp*]$^{2+}$ at the platinum electrode. A third almost reversible process corresponding to the radical trication is also observed at a more positive potential (E_0 = 0.104 V vs SCE, i_p^a/i_p^c = 0.83, 0.100 V s^{-1} scan rate). For the three redox systems, the anodic and cathodic peak separation ($E_p^a - E_p^c$) is 0.07 V with a 0.100 V s^{-1} scan rate (Table 2).

(14) Bartik, T.; Weng, W.; Ramsden, J. A.; Szafert, S.; Falloon, S. B.; Arif, A. M.; Gladysz, J. A. *J. Am. Chem. Soc.* **1998**, *120*, 11071.
(15) Bruce, M. I.; Denisovich, L. I.; Low, P. J.; Peregudova, S. M.; Ustynyuk, N. A. *Mendeleev Commun.* **1996**, 200.
(16) Coat, F.; Lapinte, C. *Organometallics* **1996**, *15*, 477.
(17) Roncali, J. *Chem. Rev.* **1997**, *97*, 173.
(18) Neenan, T. X.; Whitesides, G. M. *J. Org. Chem.* **1988**, *53*, 2489.
(19) Roger, C.; Hamon, P.; Toupet, L.; Rabaâ, H.; Saillard, J.-Y.; Hamon, J.-R.; Lapinte, C. *Organometallics* **1991**, *10*, 1045.
(20) Weyland, T.; Lapinte, C.; Frapper, G.; Calhorda, M. J.; Halet, J.-F.; Toupet, L. *Organometallics* **1997**, *16*, 2024.
(21) Denis, R.; Weyland, T.; Paul, F.; Lapinte, C. *J. Organomet. Chem.* **1997**, 545−546, 615.
(22) Le Stang, S.; Lenz, D.; Paul, F.; Lapinte, C. *J. Organomet. Chem.* **1999**, *572*, 189.
(23) Le Stang, S.; Paul, F.; Lapinte, C. *Inorg. Chim. Acta* **1999**, *291*, 403.
(24) Fermi coupling is an intramolecular process, and therefore the same splitting is expected in the solid state and in solution, as was usually observed in the other mentioned cases. In first approximation, solvation should only broaden the IR absorption peaks, and therefore at least the envelope of the Fermi doublet should be present.
(25) Connelly, N. G.; Geiger, W. E. *Chem. Rev.* **1996**, *96*, 877.

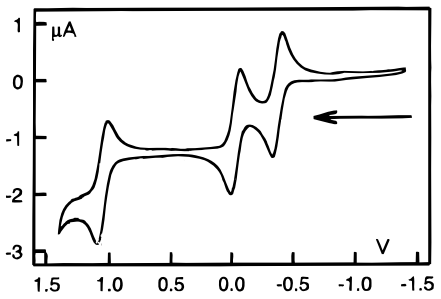

Figure 1. Cyclic voltammogram for [Cp*(dppe)Fe−C≡C-2,5-C_4H_2S−C≡C−Fe(dppe)Cp*] (**3**) in 0.1 M [nBu$_4$N][PF_6]/CH_2Cl_2 on Pt electrode; V vs SCE; scan rate 0.1 V/s; 20 °C.

Table 2. Electrochemical Data for [Cp*(dppe)Fe−C≡C−X−C≡C−Fe(dppe)Cp*][PF_6] (X = 2,5-C_4H_2S (4), −C_4− (5))'

compd	$E_{1/2}(0/+1)$,[a] V	$E_{1/2}(+1/+2)$,[a] V	ΔE, V	K_c	$E_{1/2}(+2/+3)$,[a] V
4	−0.39	−0.05	0.34	5.8×10^5	1.04
5[b]	−0.27	+0.16	0.43	2.0×10^7	0.98

[a] Cyclic voltammograms recorded in 0.1 M tetra-*n*-butylammonium hexafluorophosphate in CH_2Cl_2, 0.1 V s^{-1}, Pt electrode, V vs SCE cf. ferrocene/ferricinium 0.460 V vs SCE). [b] From ref 16.

The low values for the oxidation potentials show that these half-sandwich binuclear complexes are electron-rich compounds, as expected in the Cp*(dppe)Fe series.[2] Interestingly, the first one-electron oxidation appears at a slightly more negative potential in **4** than in **5**. The large wave separation ($|\Delta E_0| = 0.34$ V) leads to a big comproportionation constant (eq 1; $K_c = 5.8 \times 10^5$) and establishes that the MV complex **4** is stable in solution.

$$\text{Fe(II)−Fe(II)} + \text{Fe(III)−Fe(III)} \rightleftharpoons 2\text{Fe(II)−Fe(III)} \quad (1)$$

In symmetrical compounds, the potential difference ΔE_0 (or the comproportion constant K_c) is often taken as a measure of the electronic interaction through a given bridge. In fact this quantity is related to the thermodynamic stability of the MV compound described by the equilibrium of comproportion (eq 4).[2,26] It comprises other energetic terms than the through-bridge electronic interaction, like through-space electrostatic interaction, solvatation, steric interaction, or structural distortion upon electron-transfer terms. As a consequence, the K_c values indicate that the stability of the MV species increases according to the sequence **4** < **5**, but cannot be solely related to the through-bridge electronic interaction described by the electronic coupling term (V_{ab}, see below). The chemical reversibility of the oxidation processes and the large comproportionation constant obtained for **4** indicated that this compound constituted an accessible synthetic target. Thus, addition of 0.95 equiv of ferrocenium salt to a CH_2Cl_2 solution of **3** induced a fast color change from orange to dark blue. After filtration and concentration of the solution, a deep blue powder corresponding to the mixed-valence complex **4** was precipitated by addition of *n*-pentane. The crude solid was isolated in 86% yield as a thermally stable blue powder and was crystallized from a CH_2Cl_2/pentane mixture (2:1). An analytically pure sample of **4** was isolated and characterized by FTIR, Mossbauer, ESR, UV−vis, and NIR spectroscopies.

IR Spectroscopy. The bands that appear in the mid-IR from 2100 to 1700 cm^{-1} arise from the carbon−carbon triple-bond stretching modes. They are sensitive to the oxidation state of the metal center. In the mixed-valence complex **4** the spectrum reveals two distinct C≡C stretches, while only a single carbon−carbon triple-bond vibration is observed in the corresponding neutral **3** and dioxidized species $\mathbf{3}^{2+}$ (Table 1). Given the various symmetries that can be envisioned for rotamers around the central bridge (C_s or C_{2v}), two stretching modes should be observed by IR in any case. They result from the IR-active symmetric and antisymmetric combination stretches of the two symmetry-equivalent triple bonds. Even in the case of fast rotation of the terminal Cp*(dppe)Fe stoppers in solution, an averaged C_{2v} symmetry is expected for these compounds. The two resulting modes are certainly very close in energy and probably overlap, resulting in the single absorption observed bands for **3** and $\mathbf{3}^{2+}$. In this respect, it is interesting to recall that the C≡C stretch of complex **3** is split by 16 cm^{-1} in the solid, the rest of the spectrum being very similar to the solution spectrum.

IR spectroscopy has often been used to evaluate the rate of electron transfer in mixed-valence complexes when a suitable vibrator was available on one of the metallic termini. In these cases, when the electron transfer is faster than the time scale (10^{-13} s), an averaging of this specific vibrational mode is observed for the mixed-valence complex relative to the dioxidized and direduced complexes. A spectrum corresponding to the overlay of both spectra is obtained in the opposite case (i.e., slow electron transfer).[27,28] In our case, the situation is more complex since the vibrational modes involve the central bridge, and given the possibility of vibrational coupling between the C≡C motions, the symmetry of the mono-oxidized species is determinant. Assuming that the bridge remains of comparable electronic structure (i.e., polyyne-like Lewis structure), averaging can be expected with a fully delocalized electron, resulting in a symmetric structure.[29] Conversely, when the electron is localized on the time scale of the IR spectrometry, the resulting structure should belong to the less symmetric C_s group, and two separate vibrational modes should now be observed, due to the widely different electronic environment of the two acetylenic bonds. When performing a band-for-band comparison, wavenumbers recorded for Fe(II)−L−Fe(III) (**4**) are clearly different of those resulting from **3** and $\mathbf{3}^{2+}$. Alternatively, the spectrum of **4** is not an averaged spectrum of **3** and $\mathbf{3}^{2+}$. In fact, one band (1983 cm^{-1}) occupies a position intermediate between those of the pure oxidation states Fe(II)−L−Fe(II) and Fe(III)−L−Fe(III), while the second vibration is located at lower energy (1927 cm^{-1}), even below that of the mode recorded for $\mathbf{3}^{2+}$. This observation indicates that we are not in the ideal case of a fully delocalized electron. The decrease in energy of the C≡C bond stretching motion upon oxidation with respect to the

(26) Astruc, D. *Electron Transfer and Radical Processes in Transition-Metal Chemistry*; VCH: New York, 1995.

(27) Hush, N. S. *Adv. Inorg. Chem. Radiochem.* **1967**, 247.
(28) Hush, N. S. *Prog. Inorg. Chem.* **1967**, *8*, 391.
(29) Demandis, K. D.; Neyhart, G. A.; Kober, E. M.; Meyer, T. J. *J. Am. Chem. Soc.* **1998**, *120*, 7121.

Scheme 2

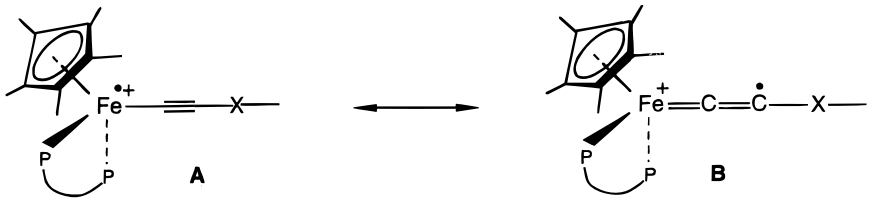

neutral complex is commonly observed in such complexes and has been rationalized lately.[30,31] The vibrational mode found at 1927 cm^{-1} seems to constitute an indication for a stronger contribution of the cumulenic limiting structure in the C≡C stretch in the MV relative to the dicationic species (Scheme 2, B). However, such a structure, which implies a participation of the spacer in the distribution of the electronic density, does not seem to be supported by the Mössbauer parameters (vide infra). The IR data do not allow ruling out the localized-electron case, but we do not favor this hypothesis since it would be in contradiction with the solvent effect on the NIR spectra. We rather believe that we are here in an intermediate situation where the electron transfer occurs after a delay close to the time resolution of the IR spectroscopy. Accordingly, it seems that the electron transfer from metal to metal takes place at an intermediate regime with a rate constant 10^{-11} s^{-1} < k_e < 10^{-13} s^{-1}.[32]

The carbon−carbon bond stretching mode of the $-C_8-$ bridge in the mixed-valence **5** exhibits one set of two bands in the mid-IR (Table 1). Here also, the observed absorptions result possibly from the overlap of several allowed modes, depending on the symmetry considered (C_{2v}, C_{2h}, or $D_{\infty h}$). A pronounced decrease of the vibrational energy upon one-electron oxidation in the series with the all-carbon spacer suggests an important reorganization of the electronic structure of the spacer associated with the oxidation of one of the termini. Again, the band observed at 1784 cm^{-1} appears at lower frequency relative to the band in the dicationic species. The presence of the same number of absorptions in the $\nu_{C\equiv C}$ region regardless of the oxidation state of the complex [Cp*(dppe)Fe−C≡C−C≡C−C≡C−C≡C−Fe(dppe)Cp*][PF_6]$_n$ (n = 0, 1) was considered as constituting an indication of the class III character of this complex.[10] However, as such, these data have to be considered with caution. The broadness of the IR band at 1784 cm^{-1} is suggestive of the presence of overlapping absorptions, possibly due to the different valence isomers evidenced by the Mössbauer spectroscopy (vide infra).[33]

UV−Vis Spectroscopy. The UV−vis spectra of the MV complexes **4** and **5** were recorded in CH_2Cl_2 (except as specified) and compared with those of the neutral corresponding derivatives. The two neutral compounds showed absorptions at λ (ϵ, M^{-1} cm^{-1}), 418 nm (40 000) for X = C_4H_2S (THF), and 389 nm (100 000), 481 nm (100 000) for X = $-C_4-$. All compounds present intense absorption below 300 nm. Their maximum could not be determined due to the solvent absorption edge, but these high-energy bands can safely be ascribed to ligand-centered $\pi-\pi^*$ electronic transitions. The broad absorption observed around 400 nm, which explains the bright orange color of this compound, may arise from metal-to-ligand charge transfer (MLCT) processes. Such transitions are also observed for mononuclear complexes in this series.[23,31]

The spectrum of the deeply colored monoradicals is very different from their neutral precursors. They display maxima in the visible range at 423 nm (8600), 588 nm (24 000), and 653 nm (28 000) for **4**, and 403 nm (56 000), 423 nm (54 000), 556 nm (70 600), 624 nm (11 000), and 707 nm (12 000) for **5**. The intense MLCT visible transition observed in the neutral complex is slightly red-shifted at 423 nm for both **4** and **5**. Additional transitions are observed above 500 nm. These transitions explain the dark green-blue color of these complexes. They might be ascribed to ligand-to-metal charge transfer (LMCT) transitions. Such transitions, which are not observed in the neutral complexes and gain in intensity in the dications,[34] are likely to take place after creation of an electronic vacancy in the HOMO after the oxidation (SHOMO).[35] Note that similar LMCTs have been observed for various Fe(III) complexes containing [Cp*(dppe)Fe(C≡C−Ar)][PF_6].[23,31] Taken as a whole, the spectra of the MV compounds **4** and **5** in the visible range present characteristic absorptions of both Fe(II) and Fe(III) alkynyl derivatives. It appears that the valence is localized for both compounds on the very fast UV−vis time scale (10^{-15} s).

Mössbauer Spectroscopy. The use of ^{57}Fe Mössbauer spectroscopy for the study of mixed-valence species is particularly interesting.[36−42] It allows the precise knowledge of iron centers, including the determination of the oxidation states, the estimation of the spin distribution between the remote ends and the organic bridge, and the evaluation of the electron-transfer rate relative to the acquisition time of the

(30) Weyland, T.; Costuas, K.; Mari, A.; Halet, J.-F.; Lapinte, C. *Organometallics* **1998**, *17*, 5569.
(31) Denis, R.; Paul, F.; Lapinte, C. Unpublished results.
(32) Ito, T.; Hamaguschi, T.; Nagino, H.; Yamaguschi, T.; Kido, H.; Zavarine, I. S.; Richmond, T.; Washington, J.; Kubiak, C. P. *J. Am. Chem. Soc.* **1999**, *121*, 4625.
(33) One referee suggested to us that the broadness of the corresponding IR band in solution could also be explained by the presence of valence isomers in solution, where internal rotations, counterion positions, and solvation should be frozen at the electronic time scale and possibly also at the vibrational time scale.
(34) Le Stang, S.; Paul, F.; Lapinte, C. Unpublished results.
(35) Grosshenny, V.; Harriman, A.; Hissler, M.; Ziessel, R. *Platinum Metals Rev.* **1996**, *40*, 26.
(36) Greenwood, N. N. *Mössbauer Spectroscopy*; Chapman and Hall: London, 1971.
(37) Dong, T.-Y.; Hendrickson, D.; Pierpont, C. G.; Moore, M. F. *J. Am. Chem. Soc.* **1986**, *108*, 963.
(38) Moore, M. F.; Wilson, S. R.; Cohn, M. J.; Dong, T. Y.; Kampara, T.; Hendrickson, D. N. *Inorg. Chem.* **1985**, *24*, 4559.
(39) Dong, T.-Y.; Kampara, T.; Hendrickson, D. N. *J. Am. Chem. Soc.* **1986**, *108*, 5857.
(40) Kampara, T.; Hendrickson, D. N.; Dong, T.-Y.; Cohn, M. J. *J. Chem. Phys.* **1987**, *86*, 2362.
(41) Le Vanda, C.; Cowan, D. O.; Leitch, C.; Bechgaard, K. *J. Am. Chem. Soc.* **1974**, *96*, 6788.

Table 3. ^{57}Fe Mössbauer Parameters[a] for [Cp*(dppe)Fe−C≡C−X−C≡C−Fe(dppe)Cp*][PF$_6$] (X = 2,5-C$_4$H$_2$S (4), −C$_4$− (5))'

compds (T)	QS (IS) mm s^{-1}			
	Fe(II)	Fe(averaged)	Fe(III)	relative areas
4 (80 K)		1.444 (0.212)		0/100/0
4 (4.5 K)		1.457 (0.212)		0/100/0
5 (293 K)[b]	1.81 (0.16)	1.35 (0.14)	0.88 (0.11)	15/70/15
5 (80 K)[b]	1.91 (0.24)	1.45 (0.21)	1.09 (0.19)	21/58/21
5 (4.5 K)[b]	1.85 (0.27)	1.40 (0.26)	1.05 (0.21)	24/52/24

[a] The velocity scale is referenced to iron metal. [b] The deconvolution was made assuming the same relative surface areas for the iron(II) and iron(III) sites.

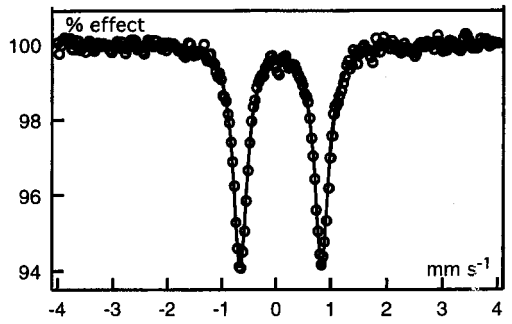

Figure 2. ^{57}Fe Mössbauer spectrum for [Cp*(dppe)Fe−C≡C-2,5-C$_4$H$_2$S−C≡C−Fe(dppe)Cp*][PF$_6$] (**4**) at 77 K. The velocity scale is referenced to iron metal.

technique.[43] Indeed, for a bis-iron MV compound, the presence of two distinct doublets in the spectrum is diagnostic of a localized valence with a rate constant $k_e > 10^{-6}$ s^{-1}, whereas observation of a single averaged doublet is diagnostic of detrapped valence with $k_e < 10^{-9}$ s^{-1}.[44]

The Mössbauer spectra of the MV compounds **4** and **5** were run at 77 K and least-squares fitted with Lorentzian line shapes.[45] The quadrupole splitting (QS) and isomer shift (δ) parameters are given in Table 3. The spectrum of the MV complex **4** exhibits a single doublet (Figure 2), and its QS parameter (Table 3) is the averaged value between the QS usually observed in the Cp*(dppe)Fe series for iron(II) ($\Delta E_Q \approx 2.0$ mm s^{-1}) and iron(III) ($\Delta E_Q \approx 0.9$ mm s^{-1}).[2,19,46−48] The odd electron should be mainly delocalized on the two metal-centered orbitals, and as a consequence, the spin density on the π-orbitals of the bridging ligand should remain in the MV as low as in the ethynyl ligand of the mononuclear iron(III) related compounds (Scheme 2, structure A).[30,31] As the two iron centers are equivalent, it could also be concluded that electron-transfer frequency from one metal site to the other is smaller than 10^{-9} s^{-1} in compound **4**. Furthermore, the Mössbauer spectrum recorded at 4.5 K still shows the presence of a sharp single doublet, indicating that the odd electron is delocalized on both metal centers on the Mössbauer time scale even at very low temperature.

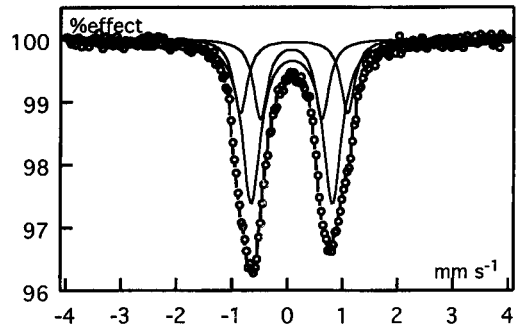

Figure 3. ^{57}Fe Mössbauer spectrum for [Cp*(dppe)Fe−C≡C−C≡C−C≡C−C≡C−Fe(dppe)Cp*][PF$_6$] (**5**) at 77 K. The velocity scale is referenced to iron metal. The deconvolution was made assuming the same relative surface areas for the iron(II) and iron(III) sites.

In contrast with complex **4**, the Mössbauer spectrum of complexes **5** displayed a broad signal corresponding to the components of the two trapped valence Fe(II) and Fe(III), together with an averaged doublet corresponding to the detrapped form (Figure 3, Table 3). Note that once again, the QS of the averaged iron is exactly the averaged value between the QS of the Fe(II) and Fe(III) in the trapped form. This indicates that the all-carbon chain as well the 2,5-bis(ethynyl)thiophene should not participate significantly in the delocalization of the spin density. As the temperature decreases from 293 to 4.5 K, the general aspect of the spectrum remains unchanged, but the ratio of trapped to detrapped valence increases from 30:70 to 48:52.

The difference of behavior of the MV complexes **4** and **5** is surprising, but would agree with the IR observations. The simultaneous observation of the trapped and detrapped forms for a given MV derivative is rare but not unprecedented. In the biferrocenium series, the presence of two polymorphs of the MV monocation have been found in the solid; one is valence-trapped, while the other is detrapped.[44] The rate of intramolecular electron transfer in mixed-valence species is extremely sensitive to the perturbation of the environment caused by differences in the crystal packing arrangements. Interactions between neighboring MV cations or with anions have pronounced effects on the electronic structure and rate of the intramolecular electron transfer.[49] The position of the counteranion located in a centrosymmetric position or not with respect to the metal centers may have a dramatic influence on the electron-transfer rate.[50] Therefore, it appears likely that the origin of the presence of two types of MV in **5** results from the difference of packing arrangements of the molecules in the solid state. Comparatively, the 2,5-bis(ethynyl)-thiophene appears to prevent more efficiently than the octatetraynediyl the formation of localized polymorph in the solid state.

ESR Spectroscopy. The X-band ESR spectra were run at 77 K in a rigid glass ($CH_2Cl_2/C_2H_4Cl_2$, 1:1) for samples of **4** and **5**. The spectra display three features

(42) Le Vanda, C.; Bechgaard, K.; Cowan, D. O. *J. Org. Chem.* **1976**, *41*, 2700.
(43) Gütlich, P.; Link, R.; Trautwein, A. *Mössbauer Spectroscopy and Transition Metal Chemistry*; Springer-Verlag: Berlin, 1978; Vol. 3.
(44) Webb, R. J.; Geib, S. J.; Staley, D. L.; Rheingold, A. L.; Hendrickson, D. N. *J. Am. Chem. Soc.* **1990**, *112*, 5031.
(45) Varret, F.; Mariot, J.-P.; Hamon, J.-R.; Astruc, D. *Hyperfine Interact.* **1988**, *39*, 67.
(46) Hamon, P.; Hamon, J.-R.; Lapinte, C. *J. Chem. Soc., Chem. Commun.* **1992**, 1602.
(47) Hamon, P.; Toupet, L.; Hamon, J.-R.; Lapinte, C. *Organometallics* **1992**, *11*, 1429.
(48) Guillaume, V.; Thominot, P.; Coat, F.; Mari, A.; Lapinte, C. *J. Organomet. Chem.* **1998**, *565*, 75.
(49) Webb, R. J.; Dong, T.-Y.; Pierpont, C. P.; Boone, S. R.; Chadha, R. K.; Hendrickson, D. N. *J. Am. Chem. Soc.* **1991**, *113*, 4806.
(50) Dong, T.-Y.; Sohel, C.-C.; Hwang, M.-Y.; Lee, T. Y.; Yeh, S.-K.; Wen, Y.-S. *Organometallics* **1992**, *11*, 573.

Table 4. ESR Data[a] for [Cp*(dppe)Fe−C≡C−X−C≡C−Fe(dppe)Cp*][PF$_6$] (X = 2,5-C$_4$H$_2$S (4), −C$_4$− (5)) and Related Compounds

X	g_{iso}	g_1	g_2	g_3	Δg	ref
4-C$_6$H$_5$	2.156	1.975	2.033	2.460	0.485	30
2,5-C$_4$H$_2$S (**4**)	2.053	2.006	2.039	2.113	0.107	this work
−C$_4$− (**5**)	2.054	1.999	2.054	2.108	0.109	this work
1,3-C$_6$H$_4$ (**6**)	2.170	1.975	2.032	2.505	0.530	30
1,4-C$_6$H$_4$ (**7**)	2.091	2.031	2.043	2.199	0.168	54
none (**8**)	2.102	2.079	2.089	2.139	0.060	8

[a] At 77 K in $CH_2Cl_2/C_2H_4Cl_2$ (1:1) glass.

corresponding to the three components of the g tensor as expected for d^5 low-spin iron(III) in pseudooctahedral geometry.[51] The g values extracted from the spectra are collected in Table 4, together with some g values from the literature for compounds of the same Cp*(dppe)Fe. Some weak and broad additional signals were also systematically observed for the complexes **5**. The resolution of all spectra was not good enough to allow the observation of the hyperfine coupling with the phosphorus nuclei, and consequently, definitive evidence for the delocalization of the MV compounds on the ESR time scale could not be obtained. For MV compounds of the biferrocenium series, it has been suggested that the anisotropy of the signal ($\Delta g = g_1 - g_3$) decreases as the rate of the intramolecular electron transfer increases, and Δg can be used to determine whether this rate is greater or not than the ESR time scale (10^{-9} to 10^{-10} s).[37,50]

From Table 4, the Δg values are significantly larger for the closely related mononuclear iron(III) complex [Cp*(dppe)Fe(C≡C−C$_6$H$_5$)][PF$_6$][52] and for the trapped mixed-valence complex [Cp*(dppe)Fe−C≡C-1,3-C$_6$H$_4$−C≡C−Fe(dppe)Cp*][PF$_6$][53] (**6**) than for the compounds **4** and **5**. Moreover, the complex [Cp*(dppe)Fe−C≡C-1,4-C$_6$H$_4$−C≡C−Fe(dppe)Cp*][PF$_6$] (**7**), which is a less strongly coupled MV than **4** and **5**, shows a slightly greater g-tensor anisotropy than **4** and **5**.[54] Accordingly, the strongly coupled MV complex [Cp*(dppe)Fe−C≡C−C≡C−Fe(dppe)Cp*][PF$_6$] (**8**) shows the weaker Δg value of this series.[8] If we assume that in the homogeneous family of MV compounds with the Cp*(dppe)Fe as terminal ends the smaller the g-tensor anisotropy, the greater the intramolecular electron transfer, it can be concluded that the electron-transfer rate is larger in the C$_4$-bridged complex **8** and decreases according to the sequence **8** > **4** ≈ **5** > **7** > **6**. Thus, isolated in a glass, the 2,5-bis(ethynyl)thiophene and 1,8-octatetraynediyl spacers appear to have a very similar efficiency for conveying electrons between the redox active Cp*(dppe)-Fe remote ends.

NIR Spectroscopy. To assess further the extent of the electronic interaction between the two coupled Cp*(dppe)Fe units in the complexes **4** and **5**, intervalence charge transfer (ICT) spectra were examined. Bands were found in the near-IR region for the two compounds (Figures 4 and 5). These bands are not present in the corresponding neutral and dioxidized species. Interestingly, the K_c values are large enough

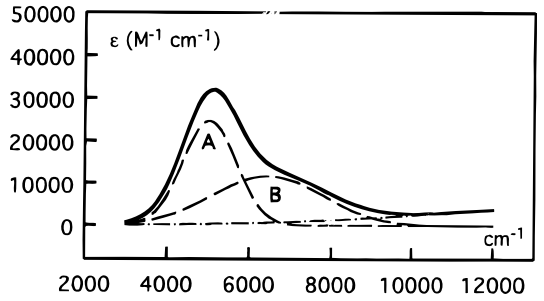

Figure 4. NIR absorption spectral data for **4** (solid line) in CH_2Cl_2 and the deconvoluted ICT bands (dashed lines). The dash−dotted line corresponds to the tail of the LMCT band.

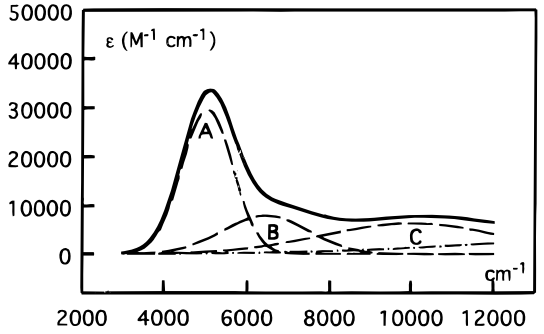

Figure 5. NIR absorption spectral data for **5** (solid line) in CH_2Cl_2 and the deconvoluted ICT bands (dashed lines). The dash−dotted line corresponds to the tail of the LMCT band.

Table 5. Solvent Effect on the NIR Spectra of the Mixed-Valence Complexes [Cp*(dppe)Fe−C≡C−X−C≡C−Fe(dppe)Cp*][PF$_6$] (X = 2,5-C$_4$H$_2$S (4), −C$_4$− (5))

compd	solvent	ν_{max} (cm^{-1})
4	CH_2Cl_2	5070
4	acetone	5154
4	CH_3CN	5186
4	CH_3OH	5208
5	CH_2Cl_2	5107
5	acetone	5163
5	CH_3CN	5157
5	CH_3OH	5208

to avoid corrections of the intensity of the bands to account for the equilibrium of comproportionation (eq 1). Moreover, the high chemical stability of these mixed-valence complexes in solution favors an accurate measurement of the intervalence bands. In the two cases, the bands display a complex shape with a single maximum and shoulders. The solvent dependence of the ICT band maximum was investigated in methylene dichloride, acetone, acetonitrile, and methanol. The increases of ν_{max} with the polarity of the solvents are 138 and 101 cm^{-1} for **4** and **5**, respectively (Table 5). This is a weak variation which can be characteristic of class III MV.[55] Indeed, the solvent dependence of the ICT bands for class II derivatives are usually much larger. In this latter case shifts of more than 1000 cm^{-1} were observed.[56] The effect of solvent on the ICT transition is a function of the outer sphere Franck−Condon activation energy for the thermal electron

(51) Rieger, P. H. *Coord. Chem. Rev.* **1994**, *135/136*, 203.
(52) Connelly, N. G.; Gamasa, M. P.; Gimeno, J.; Lapinte, C.; Lastra, E.; Maher, J. P.; Le Narvor, N.; Rieger, A. L.; Rieger, P. H. *J. Chem. Soc., Dalton Trans.* **1993**, 2575.
(53) Weyland, T.; Lapinte, C. Work in progress.
(54) Le Narvor, N.; Lapinte, C. *Organometallics* **1995**, *14*, 634.
(55) Creutz, C.; Taube, H. *J. Am. Chem. Soc.* **1969**, *91*, 3988.
(56) Callahan, R. W.; Brown, G. M.; Meyer, T. J. *J. Am. Chem. Soc.* **1974**, *96*, 7827.

Table 6. Gaussian Analysis and Summary of the Electronic Spectral Data for the ICT Bands[a] of the Mixed-Valence Complexes [Cp*(dppe)Fe−C≡C−X−C≡C−Fe(dppe)Cp*][PF$_6$] (X = 2,5-C$_4$H$_2$S (4), −C$_4$− (5), X = None, 8)

compd/band	ν_{max} (cm^{-1})	ϵ_{max} (M^{-1} cm^{-1})	$\Delta\nu_{1/2}^{exp}$ (cm^{-1})	$\Delta\nu_{1/2}^{calc}$ (cm^{-1})	$d_{(Fe\ Fe)}$ (Å)	V_{ab}[b] (cm^{-1})	V_{ab}[c] (cm^{-1})
4 band A	5030	25000	1500	3400	11.6	773	2515
band B	6450	11700	3200	3900		1356	
5 band A	5040	30000	1500	3400	12.6	778	2520
band B	6450	7900	1200	3900		682	
band C	10000	6400	5000	4800		1561	
8[d]	7541	12000	3250	4220	7.436		3790

[a] In CH_2Cl_2. [b] Calculated from Hush formula for a class II compound [V_{ab} (cm^{-1}) = $(0.0205/r)(\epsilon_{max}\Delta\nu_{1/2}\nu_{max})^{1/2}$; r = distance between the redox centers in Å]. [c] Calculated for a class III MV [V_{ab} (cm^{-1}) = $\nu_{max}/2$]. [d] From ref 8.

transfer. Therefore, in the case of **4** and **5**, it can be stated that the intramolecular electron transfer is expected to be rapid on the time scale of solvent molecule reorganization for these three compounds in solution ($\sim 10^{-12}$ s), and as a consequence, the solvation sphere of both redox centers must be relatively symmetric.[57]

As shown in Figures 4 and 5, the shape of the bands is complex and the determination of their positions, widths, and intensities is not straightforward. Assuming that the ICT bands consist of Gaussian band shapes, the spectra were deconvoluted in the range 4000−12 000 cm^{-1}.[58] In our case, the full observation of the major component of the spectrum (band A), the distinct identification of a shoulder in the main peak, and the presence of a well-defined second maximum in the spectrum of **5** greatly facilitate the deconvolution process. The results are sufficiently good to allow an exact overlying of the sum of the spectral components with the experimental spectra after filtration of the noise and residual vibration due to the solvent subtraction. Table 6 summarizes spectral data extracted from the ICT band shape analysis. For the two compounds, the MLCT bands observed in the visible and ultraviolet region tail in the NIR range. The traces of these residual absorptions are shown in Figures 4 and 5, but the corresponding spectral data are not listed in Table 6. The Gaussian analysis of the ICT bands of both compounds gave very similar data with two bands (A and B) at almost the same position. In the case of the MV with the −C$_8$− bridge a third component is located at higher energy (band C). For the two complexes, the band A, which constitutes the major component of the spectrum, is significantly narrower than what Hush's theory would predict (see Table 6). Again, this is in agreement with the class III character for these MV compounds. In contrast, the width obtained for the components B and C, located at higher energy, fits very well with the value calculated for class II systems.[59]

The deconvolution of the experimental spectra constitutes a useful tool for a comprehensible description of the NIR spectra of the MV complexes, allowing an accurate determination of the position, width, and intensity of the bands, but the physical significance of the multiple Gaussian-shape absorption bands is not clear. The presence of several NIR bands in the spectrum of MV complexes is not uncommon. Accordingly, the class II and III diosmium and osmium/ruthenium mixed-valence complexes exhibit two or three NIR bands due to spin−orbit coupling.[60−62] Multiple absorptions were also observed in the case of the closely related mixed-valence complex [Cp*(NO)(PPh$_3$)Re−C≡C−C≡C−Re(PPh$_3$)(NO)Cp*][PF$_6$], and spin−orbit coupling was considered to be the most likely explanation.[11] This effect is much more pronounced for third-row transition metals, but cannot be completely ruled out for iron complexes. However, we do not believe this to be a likely explanation. Indeed, while the general aspect of the NIR spectra of these two MVs is very similar, they only differ by the presence of a third band in the spectrum of **5**. Thus, the different number of bands in the NIR spectrum of **4** and **5** seems to be clearly related to the structure of the spacer and not to the metal termini.

The ICT bands correspond to bridge-mediated electron transfer from Fe(II)−L−Fe(III)$^{\bullet+}$ to Fe(III)$^{\bullet+}$−L−Fe(II). As the terminal metal sites are equivalent, the differences between the two NIR spectra should reveal the role played by the π-system of the bridges in the electronic coupling between the remote ends. Assuming that band A can be attributed to bridge-mediated superexchange[63] between the strongly coupled iron sites, the origin of the bands B and C remains open to question. In the case of long-distance bridge-mediated electron transfer, it cannot be excluded that, beside the superexchange mechanism, other processes competitively occur. Thus, the double exchange mechanism was also proposed.[64,65] This second mechanism becomes more probable as the bridge length and the level of the π-orbitals increase. Moreover, effects of bridge redox state levels on the electron transfer have recently been proposed to explain the rich absorption spectrum of purely organic mixed-valence compounds.[66]

The NIR bands can be used to determine the electronic coupling parameters V_{ab} (also denoted H_{ab}).[26] The significance and determination of this parameter are quite different for class II and class III mixed-valence systems. According to the criteria of bandwidth defined

(57) Demadis, K. D.; Meyer, T. J.; White, P. S. *Inorg. Chem.* **1997**, *36*, 5678.

(58) Reimers, J. R.; Hush, N. S. *Inorg. Chem.* **1990**, *29*, 4510.

(59) Comparison of the envelope of the ICT bands of **4**, recorded in CH_2Cl_2 and CH_3CN, clearly shows that the position of the band B is much more sensitive to the solvent polarity than that band A is. This strongly supports the class II and class III character of the ICT corresponding to the bands B and A, respectively.

(60) Kober, E. M.; Goldsby, K. A.; Narayane, D. N. S.; Meyer, T. J. *J. Am. Chem. Soc.* **1983**, *105*, 4303.

(61) Lay, P. A.; Magnuson, R. H.; Taube, H. *Inorg. Chem.* **1988**, *27*, 2364.

(62) Laidlaw, W. M.; Denning, R. G. *J. Chem. Soc., Dalton Trans.* **1995**, 1987.

(63) "The term superexchange in ET literature is generally meant to imply the mixing of the donor and acceptor states by a virtual electronic state of the bridging species. In particular, usage of the term generally implies that neither electron nor hole is ever vibronically localized on the bridge."[66,75]

(64) Richardson, D. E.; Taube, H. *J. Am. Chem. Soc.* **1983**, *105*, 40.

(65) Halpern, J.; Orgel, L. E. *Discuss. Faraday Soc.* **1960**, *29*, 32.

(66) Nelsen, S. F.; Ismagilov, R. F.; Powell, D. R. *J. Am. Chem. Soc.* **1998**, *120*, 1924.

by Hush, the V_{ab} parameters determined from the bands A were calculated using the formula established for class III MV, and the V_{ab} values corresponding to the bands B and C were calculated with the relationship derived from Hush's theory (see Table 6). Nonetheless, to facilitate comparisons with other literature data, V_{ab} values corresponding to band A are also given using the class II formula (Table 6). Interestingly, the V_{ab} parameters determined for band A are identical for compounds **4** and **5**. As a result, it appears that the X groups 2,5-C_4H_2, and $-C_4-$ provide efficient and very similar through-bridge electronic coupling (i.e., superexchange) in these MV complexes for the most efficient pathway. In terms of electronic coupling, the difference between these two compounds mainly deals with the contribution of secondary pathways which have not been clearly delineated.

The electron transfer in symmetrical intervalence systems is furthermore characterized by the vertical reorganization energy ($\lambda = h\nu$).[26] Depending on the MV class a compound belongs to, the meaning of this parameter is very different. In the class III model, the diabatic surface energy is two parabolas both centered at 0.5 on the reaction coordinate and their separation at the ground state is the optical energy (λ), which is also 2 times the electronic coupling (V_{ab}). Class II compounds, on the other hand, obey the Marcus−Hush model.[28,67−69] The parabolas are centered at 0 and 1 on the electron-transfer coordinate, and their energy separation at the ground-state minimum is λ. This is a vertical transition due to the Franck−Condon principle. According to this scheme, the optical energy λ rapidly increases when the distance between the two redox centers A and B located at 0 and 1 slowly increases. Comparison of the energies of the optical transition determined for the series of complexes **4** and **5**, in which the metal centers are separated by similar nanoscopic distances, with that previously observed for the related complex [Cp*(dppe)Fe−C≡C−C≡C−Fe(dppe)Cp*][PF_6] (**8**), in which the separation between the metal ends is less than 7.5 Å, reveals that the optical energies decrease while the distance between the redox active centers increases. This effect of the distance on the optical energy is not compatible with the class II model, but would be in agreement with the class III character for **4**, **5**, and **8**. Comparison of our observations with those obtained in the well-known series of mixed valence $[(NH_3)_5M-L-M(NH_3)_5]^{5+}$ (M = Ru, Os) shows a different behavior. It has been shown that depending on L, the MV complexes belong either to class III (L = pyrazine) or to class II (L = 1, 4-bipyridine). It has also be reported that the ICT bands are observed at lower energy for L = pyrazine than for L = 1,4-bipyridine.[55,56]

Finally, introduction of a thiophene group in the $-C_4-$ carbon chain constitutes an attractive means for the size-expansion of molecular wires. In comparison with the $-C_8-$ spacer, the synthesis is greatly facilitated and the electron conduction at the molecular level is apparently not affected. Noteworthy, class III mixed-valence compounds with nine bonds (or more) between the redox active sites are quite rare.[70] Moreover, in our series, it appears that the presence of the C_4H_2S group in the linear spacer gives more appropriate molecular arrangements in the solid state for efficient intramolecular electron transfer. Combination of linear carbon chains with thiophene and polythiophene groups for the realization of molecular devices will be the subject of future reports from this laboratory.

Experimental Section

General Data. Reagent grade diethyl ether, toluene, and pentane were dried and distilled from sodium benzophenone ketyl prior to use. Pentamethylcyclopentadiene was prepared according to the published procedure,[71] and other chemicals were used as received. All manipulations were carried out under an argon atmosphere using Schlenk techniques or in a Jacomex 532 drybox filled with nitrogen. Routine NMR spectra were recorded using a Bruker DPX 200 spectrometer. High-field NMR spectra experiments were performed on a multinuclear Bruker WB 300 instrument. Chemical shifts are given in parts per million relative to tetramethylsilane (TMS) for ^{1}H and ^{13}C NMR spectra and H_3PO_4 for ^{31}P NMR spectra. Cyclic voltammograms were recorded using a PAR 263 instrument. Transmittance-FTIR spectra were recorded using a Bruker IFS28 spectrometer. UV−vis spectra were recorded on a UVIKON spectrometer. X-band ESR spectra were recorded on a Bruker ESP-300E spectrometer at 77 K in liquid nitrogen. An Air Products LTD-3-110 liquid helium transfer system was attached for the low-temperature measurements. The ^{57}Fe Mössbauer spectra were obtained by using a constant acceleration spectrometer previously described with a 50 mCi ^{57}Co source in a Rh matrix.[72] The sample temperature was controlled by an Oxford MD306 cryostat and an Oxford ITC4 temperature controller. Computer fitting of the Mössbauer data to Lorentzian line shapes was carried out with a previously reported computer program.[45,73] The isomer shift values are reported relative to iron foil at 298 K and are not corrected for the temperature-dependent second-order Doppler shift. The Mössbauer sample cell consists of 2 cm diameter cylindrical plexiglass holder. Liquid NIR spectra were recorded on a Cary 5 spectrometer. Elemental analyses were performed at the Centre for Microanalyses of the CNRS at Lyon-Solaise, France.

Synthesis of [{Fe(η^5-C_5Me_5)(η^2-dppe)(C≡C−)}$_2${2,5-C_4H_2S}]. In a Schlenk flask wrapped with aluminum foil, 87 mg (0.32 mmol) of 2,5-bis(trimethylsilylethynyl)thiophene in 40 mL of methanol was stirred overnight in the presence of 2.2 equiv of potassium carbonate (97 mg, 0.70 mmol). Then 2 equiv of [Fe(η^5-C_5Me_5)(η^2-dppe)Cl] (400 mg, 0.64 mmol) and 2.2 equiv of $NaBPh_4$ (241 mg, 0.70 mmol) were added. After approximatively 8 h of stirring an excess of KOBu^t (79 mg, 0.70 mmol) was introduced. The agitation was maintained for 2 h before the solvent was removed under vaccum. The residue was extracted with toluene (4 × 10 mL), and the solution was evaporated to dryness. The solid was washed by pentane (3 × 10 mL) and dried in vacuo to give 373 mg (0.29 mmol, 72%) of [{Fe(η^5-C_5Me_5)(η^2-dppe)(C≡C−)}$_2${2,5-C_4H_2S}] as an orange powder. Anal. Calcd for $C_{80}H_{80}Fe_2P_4S_1\cdot H_2O$: C, 72.40; H, 6.23. Found: C, 72.40; H, 6.11. DSC ($T_i/T_e/T_p$) 191/244/334 °C.[74] FT-IR (Nujol, cm^{-1}): ν 2054 (s, C≡C); 2039 (s, C≡C). FT-IR (CH_2Cl_2, cm^{-1}): ν 2041 (s, C≡C). ^{31}P NMR (121 MHz, C_6D_6): δ_P 100.5 (s, dppe). ^{1}H NMR (200 MHz, C_6D_6): δ_H 8.11−7.00 (m, 40H, 4 C_6H_5); 6.64 (s, 2H, C_4H_2S); 2.64; 1.81 (2m, 8H,

(67) Marcus, R. A.; Sutin, N. *Biochim. Biophys. Acta* **1985**, *811*, 265.
(68) Marcus, R. A. *Discuss. Faraday Soc.* **1960**, *29*, 21.
(69) Hush, N. S. *Trans. Faraday Soc.* **1961**, *57*, 557.
(70) Evans, C. E. B.; Yap, G. P. A.; Crutchley, R. J. *Inorg. Chem.* **1998**, *37*, 6161.
(71) Kohl, F. X.; Jutzi, P. *J. Organomet. Chem.* **1983**, *243*, 119.
(72) Boinnard, D.; Bousseksou, A.; Dworkin, A.; Savariault, J.-M.; Varret, F.; Tuchagues, J.-P. *Inorg. Chem.* **1994**, *33*, 271.
(73) *International Conference on Mössbauer Effect Applications*; Varret, F., Varret, F., Eds.; Indian Science Academy, New Delhi, 1982; Jaipur, India, 1981.

CH_{2dppe}); 1.53 (s, 30H, $C_5(CH_3)_5$). ^{13}C NMR (75 MHz, C_6D_6): δ_C 140.2−127.4 (m, Ph_{dppe}); 139.2 (t, $^2J_{PC}$ = 40 Hz, Fe−*C*≡C); 127.3 (m, $C_4H_2S/C_{2,5}$); 124.5 (dd, $^1J_{CH}$ = 165 Hz, $^2J_{CH}$ = 6 Hz, $C_5H_2S/C_{3,4}$); 112.9 (m, Fe−C≡*C*); 88.0 (s, $C_5(CH_3)_5$); 31.2 (m, CH_{2dppe}); 10.5 (q, $^1J_{CH}$ = 126 Hz, $C_5(CH_3)_5$).

Synthesis of [{Fe(η^5-C_5Me_5)(η^2-dppe)(C≡C)}$_2${2,5-C_4H_2S}][PF_6]. [Fe(η^5-C_5H_5)$_2$][PF_6] (0.053 g, 0.16 mmol, 0.95 equiv) was added to a solution of [{Fe(η^5-C_5Me_5)(dppe)(C≡C)}$_2${2,5-C_4H_2S}] (0.339 g, 0.49 mmol) in CH_2Cl_2 (20 mL). The orange mixture became immediatly blue and was stirred for 2 h at room temperature. The solution was filtered and concentrated in vacuo to ∼15 mL. Addition of 50 mL of *n*-pentane allowed precipitation of a solid. After decantation and subsequent washings with 10 mL of ether and 10 mL of pentane, drying under vacuum yielded the pure [{Fe(η^5-C_5Me_5)(dppe)(C≡C)}$_2$-{2,5-C_4H_2S}][PF_6] as a blue powder (0.200 g, 86%). Crystallization from a CH_2Cl_2/pentane mixture (2:1) provided pure microcrystals (72%). Anal. Calcd for $C_{80}H_{80}F_6Fe_2P_5S_1$: C, 66.08; H, 5.55. Found: C, 65.87; H, 5.51. FT-IR (Nujol, cm^{-1}): ν 1977 (s, C≡C); 1910 (s, C≡C); 839 (s, P−F). FT-IR (CH_2Cl_2, cm^{-1}): ν 1983 (m, C≡C); 1927 (s, C≡C); 847 (s, P−F).

(74) DSC parameters (T_i, initial peak temperature; T_e, extrapolated peak-onset temperature; T_p, maximum peak temperature). See ref 76.
(75) Kosloff, R.; Ratner, M. A. *Isr. J. Chem.* **1990**, *30*, 45.
(76) Cammenga, H. K.; Epple, M. *Angew. Chem., Int. Ed. Engl.* **1995**, *34*, 1171.

Acknowledgment. We are grateful to Dr. F. Coat for the pioneering work on compound **5** and A. Mari (LCC, Toulouse) for Mössbauer measurements; we are also indebted to ANRT and Laboratoires Standa (Caen) for financial support to S.L.S. We thank one of the reviewers for his very valuable comments.

OM9908231